PROCEEDINGS OF SCIENCE

The number of muons measured in hybrid events detected by the Pierre Auger Observatory

Maximilian Stadelmaier[a,*] **for the Pierre Auger**[b] **Collaboration**

[a] *Institute of Physics of the Czech Academy of Sciences, Na Slovance 1999/2, 18200 Prague, Czech Republic*
[b] *Observatorio Pierre Auger, Av. San Martín Norte 304, 5613 Malargüe, Argentina*

E-mail: spokespersons@auger.org

The number of muons produced in extensive air showers is a reliable proxy for the amount of hadron production that occurs during the shower development. It is, therefore, an important observable in the context of identifying the mass composition of ultrahigh-energy cosmic rays. Beyond LHC energies, however, hadronic multiparticle production as it occurs in air showers from ultrahigh-energy cosmic rays, is poorly understood, and currently there is little to no way to directly test it experimentally. In simulations, current models of hadronic interactions are unable to produce the average number of muons that is measured by multiple air-shower experiments. In this work, we estimate the number of muons in vertical hybrid events detected by both the fluorescence and surface detectors of the Pierre Auger Observatory above a primary energy of 3 EeV. To reconstruct the signal, we use a model of the water-Cherenkov detector responses that is based on air-shower universality. We take into account the effect of the longitudinal shower development on the lateral distribution of the signal at the ground, as well as the primary energy estimated from the calorimetric energy deposition of the air shower. In this way, we are able to estimate the amount of muons created in vertical showers, relative to expectations from simulated showers using modern hadronic interaction models.

38th International Cosmic Ray Conference (ICRC2023)
26 July - 3 August, 2023
Nagoya, Japan

*Speaker

PoS(ICRC2023)339

1. Introduction

The mass composition of cosmic rays evolves as a function of the primary energy, reflecting the different processes that create and accelerate particles in our galaxy and beyond. At the highest energies, the composition, as well as the origin of cosmic rays, are considered big open questions in modern physics. They are being investigated using giant detector arrays and fluorescence telescopes observing extensive air showers produced by cosmic rays [1].

The number of muons produced in extensive air showers is an important observable to study in the context of the mass composition of ultrahigh-energy cosmic rays, since it is directly related to the hadron production occurring in the shower. Previous studies at different experiments, however, failed to measure the same absolute scale of the number of muons produced in air showers over a wide range in primary energies [2]. Moreover, the number of muons produced in simulated air showers using various post-LHC models of hadronic interactions disagree with measured data and each other. It is therefore not straightforward to interpret the mass composition based on the absolute number of muons observed in data. Nevertheless, we can do so based on the assumption that the amount of hadron multiparticle production, which is the dominant source of muons in air showers, is increased in air showers induced by heavier nuclei over protons or neutral particles.

Directly detecting the muons from air showers is possible using underground muon detectors (see, for instance [3]) or analysing the data from horizontal air-shower events [4], in which the electromagnetic component has been almost completely attenuated by the atmosphere. However, estimating the number of muons from the information collected by the surface detector (SD) events only is ambitious because the lateral distribution of particles at the ground does not trivially allow for the independent reconstruction of the relative number of muons R_μ, the primary energy E_0, and the stage of development of the shower, described by the depth of the shower maximum, $X_{\max}$. In this work, we use the combined information of the hybrid detector employed by the Pierre Auger Observatory (in short *Auger*) [5] to reconstruct R_μ for vertical (zenith angle below 60°) events at high energies.

2. Method

The primary energy of cosmic rays detected by their air-shower signal in surface detector arrays is commonly estimated using the constant intensity cut (CIC) method [6]. In this way, shower fluctuations in terms of the depth of the shower maximum and the number of muons produced are not taken into account on event-by-event level [7]. However, fluorescence detector (FD) data of Auger provide a precise measurement of the individual shower development as well as an estimation of the primary energy from the calorimetric energy deposit of the air shower, that is independent from SD data. We employ a model [8] of the responses of the water-Cherenkov detectors in the Auger SD, which is parametrized using simulated air-shower events, to describe the SD data while using the FD estimation of the primary energy and the depth of the shower maximum as a input parameters. The dependence of the size of the shower footprint on the primary energy as well as the effect of the depth of the shower maximum on the lateral distribution of particles is thus taken into account. The number of muons is then the only free parameter to be fixed in a likelihood fit to describe the SD signal at the ground. Furthermore, we correct for the composition bias that is

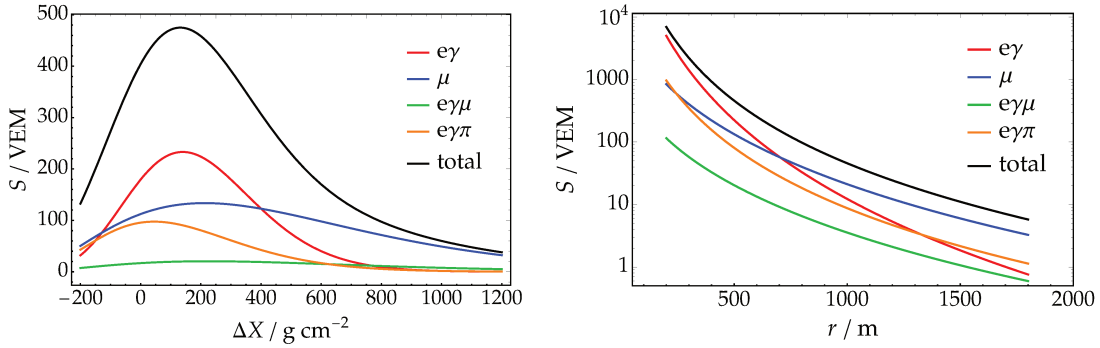

Figure 1: Model of the signal deposited in an Auger water-Cherenkov detector. The model is evaluated for a shower with a primary energy of $E_0 = 10^{19}$ eV and $R_\mu = 1$. The longitudinal development of the expected signal (*left*) is evaluated at a distance of 500 m from the shower axis; the lateral distribution of the expected signal (*right*) is evaluated for a shower with a zenith angle of $\theta = 12°$ and $X_{\max} = 700\,\mathrm{g\,cm^{-2}}$ at $\psi = \pi/2$. The signal is given in units of VEM [17].

present in the estimated number of muons when employing the primary energy estimate from the measurement of the calorimetric energy deposit. In the following, the model of the expected SD signals as well as the validation procedure using CORSIKA [9] Monte-Carlo (MC) simulations will be described.

2.1 The model of SD signals

The expected responses of the water-Cherenkov detectors of the Auger SD are described by a signal model that is motivated by air-shower universality [10–14]. We divide the particle content of an air shower into four main components. These are the electromagnetic component, $\mathrm{e}\gamma$, containing all electrons, positrons, as well as photons; the muonic component, μ, containing all muons and antimuons; the muonic-electromagnetic component, $\mathrm{e}\gamma(\mu)$, containing all electromagnetic particles produced by muon decay; and the hadronic-electromagnetic component, $\mathrm{e}\gamma(\pi)$, which contains all electromagnetic particles from hadron decays, as well as all hadrons themselves [13, 14]. Near the ground level, the lateral and longitudinal development of each component, as well as the dependence of the number of particles produced on the primary energy, can be approximately disentangled. The expected signal deposited in a detector at the ground is parametrized using a modified Gaisser-Hillas function [14], and the NKG function [15, 16], to describe the longitudinal and lateral development of the shower, respectively. For each particle component, the dependence of the shower size on the primary energy, the average longitudinal profile, as well as the average lateral profile, is parametrized individually based on simulated detector responses of proton showers. In this way, the average signal expected to be deposited in a detector from each particle component can be accurately expressed as a function of the primary energy E_0, and the geometry of the event. The parametrization of the model is described in detail in [8]. An example of the behavior of the model evaluated as a function of the slanted atmospheric distance ΔX of a detector to the shower maximum, and as a function of the distance r of a detector to the shower axis, is shown in Fig. 1.

According to the amount of hadron production occurring during the shower development, one expects a larger contribution to the absolute signal from the hadronic components (μ, $\mathrm{e}\gamma(\mu)$, $\mathrm{e}\gamma(\pi)$),

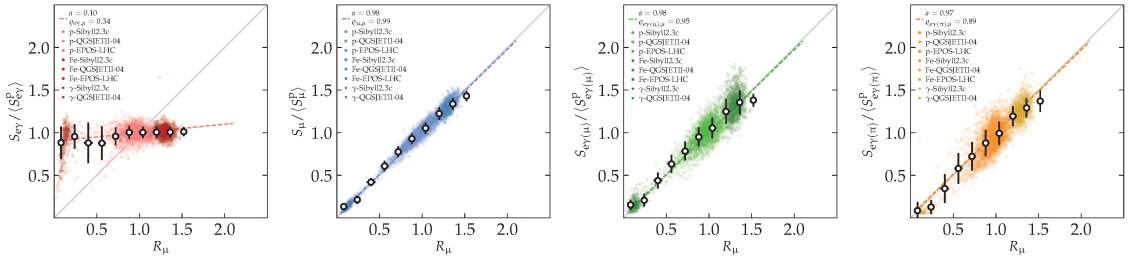

Figure 2: Ratio of simulated and parametrized signals in water-Cherenkov detectors as a function of the relative muon number R_μ for each particle component. The legend shows the correlation coefficient ϱ for each data set, as well as the slope a of the dashed line fitted to the data.

while the shower size of the eγ component is approximately constant[1]. To quantify the contribution of the hadronic components, we introduce the relative muon number R_μ. It is defined as the number of muons produced in the shower divided by the average number of muons produed in a respective proton shower of the same energy, $R_\mu = N_\mu / \langle N_\mu^{\mathrm{p}} \rangle$. The model is parametrized using a library of proton-induced showers simulated using the EPOS-LHC model of hadronic interactions [18]. Thus, for the average EPOS-LHC proton shower we expect $R_\mu = 1$, by definition. The detector simulation used for the parametrization of the model is produced by the Offline software framework [19]. An example comparison of the parametrized and simulated component signals deposited in water-Cherenkov detectors at a distance of 750 m as a function of R_μ is shown in Fig. 2 for various primary particles and hadronic interaction models. We find that the description of the SD signal of the model scaled according to R_μ of the individual showers is accurate for all primary particles and hadronic interaction models[2]. The total SD signal is well described by

$$S_{\mathrm{tot}} \simeq S_{\mathrm{e}\gamma} + R_\mu \left(S_\mu + S_{\mathrm{e}\gamma(\mu)} + S_{\mathrm{e}\gamma(\pi)} \right), \tag{1}$$

and second-order corrections for detector effects as well as for azimuthal asymmetry.

2.2 Validation and performance

The model of the shower footprint at the ground level uses the depth X_{max} of the shower maximum, the primary energy E_0, and the muon number R_μ either as input or as free parameters to describe the signal measured by the SD. In this work, we will use X_{max} and E_0 as measured by the fluorescence detector of Auger and leave only R_μ as a free parameter to fit the data. For this reason, we investigate *Golden Hybrid* events, which can be individually reconstructed by both the surface

[1] From the Heitler-Matthews model of air-showers, for a primary of nuclear mass A, on average, one expects

$$N_{\mathrm{e}\gamma}^{(A)} = \left(E_0 - A^{1-\beta} E_\mu^{(1)} \right) / \epsilon_{\mathrm{c}}^{\mathrm{e}\gamma}$$

particles being created in the eγ component, where $E_\mu^{(1)} = (E_0/\epsilon_{\mathrm{c}}^{\pi})^{\beta} \epsilon_{\mathrm{c}}^{\pi}$ is the average energy deposited in the μ component for $A = 1$; furthermore $\beta \simeq 0.95$, $\epsilon_{\mathrm{c}}^{\pi} \simeq 20\,\mathrm{GeV}$, and $\epsilon_{\mathrm{c}}^{\mathrm{e}\gamma} \simeq 87\,\mathrm{MeV}$. It is straightforward to show that $\partial N_{\mathrm{e}\gamma}^{(A)} / \partial A$ is negative but approximately 0 at high energies, $E_0 \gtrsim 3\,\mathrm{EeV}$. The spectra of electromagnetic particles are approximately independent of the cosmic-ray mass [12].

[2] We examined simulations using photon, proton, and iron primaries, using the EPOS-LHC [18], SIBYLL2.3C [20], and QGSJETII-04 [21] models of hadronic interactions.

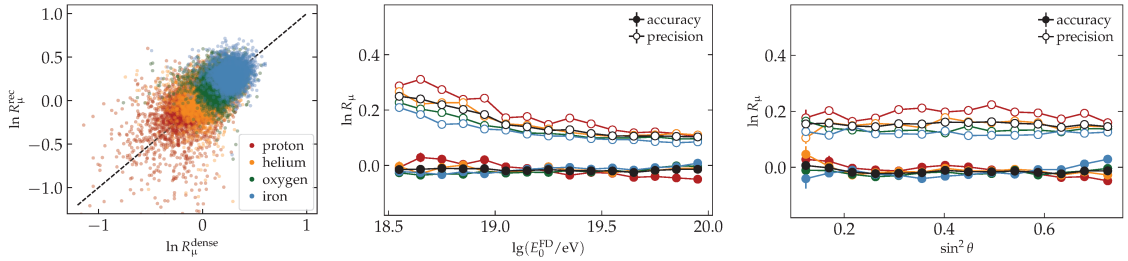

Figure 3: Correlation of reconstructed and MC values of $\ln R_\mu$ (left), as well as the precision and accuracy of the reconstructed $\ln R_\mu$ as a function of the primary energy (middle) and zenith angle (right). The colors for the individual primary particles are indicated in the left panel; black markers indicate the average over all four primary particles.

Table 1: Individual contributions to the systematic uncertainty of the reconstructed number of muons.

p	$X_{\max}$	$\vec{x}_{\text{core}}$	calib.	A	E_0	$\boldsymbol{\Sigma}$
$\sigma_{\text{sys}}(p)$	$10\,\text{g}\,\text{cm}^{-2}$	23 m	2%	0 – 56	14%	
$\sigma_{\text{sys}}(R_\mu)$	1% – 2%	1% – 3%	3%	1% – 5%	7% – 15%	**8% – 17%**

and fluorescence detector of Auger. We will use the quality criteria introduced in preceding studies to evaluate the depth of the shower maximum and the surface detector data, respectively [22, 23].

To validate the method, we use MC simulations of air-showers and reconstruct R_μ. We present the correlation of the reconstructed muon number, R_μ^{rec}, and the respective value calculated from simulated dense stations in log-scale, as well as the accuracy and precision as a function of the reconstructed primary energy and zenith angle in Fig. 3. The simulation library comprises approximately 15000 showers of each indicated primary particle, simulated with the EPOS-LHC model using a flat spectrum in $\lg(E_0/\text{eV})$ and $\sin^2\theta$. To treat the aforementioned bias caused by using the calorimetric energy deposit as a proxy for the energy of the primary particle, the reconstructed data are obtained by rescaling the raw fit result, $\ln R_\mu^{\text{rec}} \simeq 0.75 \ln R_\mu^{\text{raw}} + 0.05$. As can be seen in Fig. 3, the method provides a precise and unbiased estimate of the number of muons. We observe an improvement in the precision of the reconstructed results with increasing primary energy, while the precision as a function of the zenith angle is flat. In general, the reconstruction of $\ln R_\mu$ for heavier primary particles tends to have a slightly better precision than for lighter ones, due to the lower shower-to-shower fluctuations for heavier primaries.

3. Measurement of the number of muons

In the following, we discuss the measurement of the number of muons in Auger *Golden Hybrid* events, including systematic uncertainties and the event-level correlation of $X_{\max}$ and $\ln R_\mu$.

3.1 Systematic uncertainties

The main sources of systematic uncertainties are the uncertainties of the respective input parameters p to the signal model. We identified (in ascending order) the depth of the shower maximum, $X_{\max}$, the reconstructed shower core position $\vec{x}_{\text{rec}}$, the surface detector calibration,

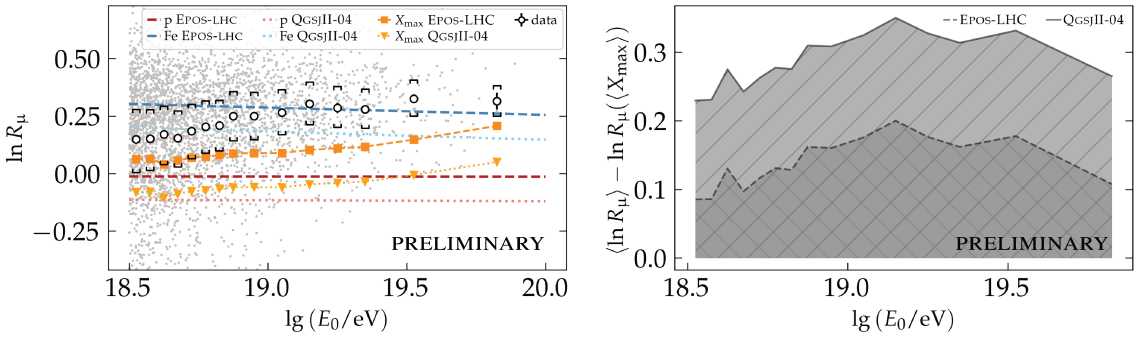

Figure 4: Left: The logarithmic muon number $\ln R_\mu$ as a function of the primary energy. Expectation values for proton and iron primaries are indicated in red and blue color, respectively, obtained from simulations using the EPOS-LHC and QGSJETII-04 models of hadronic interactions. Expectation values according to the mean values of X_{max} converted to an equivalent $\ln R_\mu$ are depicted in orange for both hadronic interaction models. The mean values of the data in the respective energy bin are depicted as a white circular marker with error bars indicating the standard deviation of the mean and error brackets indicating the systematic uncertainties. Individual events are depicted as grey markers. Right: Difference in the expected number of muons based on the depth of the shower maximum with respect to data as a function of the primary energy.

the mass composition and mean atomic mass A, and the primary energy, E_0, as contributions to systematic uncertainty of the reconstructed number of muons. The individual contributions are listed in Table 1. We reconstructed the detector data with each of the contributions altered by the respective amount and evaluated the data individually. In general, the resulting systematic uncertainty of R_μ reduces with increasing primary energy, and is approximately $^{+17\%}_{-16\%}$ at $E_0 \simeq 3\,\mathrm{EeV}$ and $^{+10\%}_{-8\%}$ at $E_0 \simeq 60\,\mathrm{EeV}$. Furthermore, we correct for seasonal variations and long-term performance effects of the detector.

3.2 The number of muons as function of the primary energy

In Fig. 4 (*left*), we present the number of muons measured as a function of the primary energy. The blue and red reference lines indicate the expectation values for showers from simulated proton and iron primary particles using the EPOS-LHC and QGSJETII-04 hadronic interaction models. At the highest energies, we observe an average number of muons larger than expected in all scenarios from hadronic interaction models. Orange markers indicate the expectation values corresponding to the respective values of X_{max}, converted to the equivalent $\ln R_\mu$ assuming a consistent interpretation of the primary mass for each hadronic interaction model. At all energies, the observed number of muons is significantly larger than expected from X_{max} measurements. In Fig. 4 (*right*), the difference between the measured and expected $\ln R_\mu$ is shown as a function of the primary energy for both hadronic interaction models. On average, we observe approximately 15% (30%) more muons than expected from X_{max} measurements when comparing to simulations using the EPOS-LHC (QGSJETII-04) model of hadronic interactions. This result is in accordance with the well-established muon puzzle - the discrepancy in the measured and expected number of muons, which was previously reported by Auger and other experiments [2, 4].

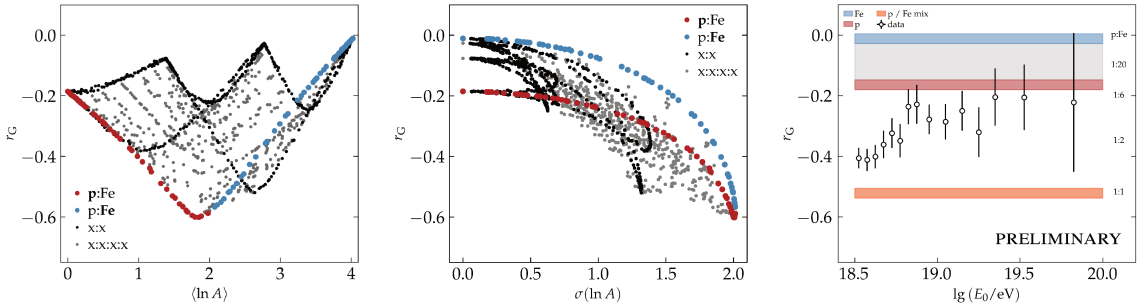

Figure 5: Left/Middle: Correlation of $X_{\max}$ and $\ln R_\mu$ in derived from simulations for various composition scenarios as a function of $\langle \ln A \rangle / \sigma(\ln A)$. Right: Correlation of $X_{\max}$ and $\ln R_\mu$ as a function of the primary energy. The orange band represents an extreme 1:1 proton-iron mix scenario, the red (blue) band depicts the expectation value for r_G for a pure proton (iron) scenario. Other pure composition scenarios are expected within the gray band. Numbers on the right indicate r_G for example proton-iron mixes from MC data.

3.3 Correlation of the number of muons with the depth of the shower maximum

Additionally to the average number of muons, we examine the correlation of the individual measured values of $X_{\max}$ and $\ln R_\mu$, which does not greatly depend on the state-of-the-art hadronic interaction models, and which is a measure for the purity of the primary beam [24]. A similar study was previously presented in [25], where the normalized surface detector signal at a distance of 1000 m from the shower core was used as a proxy for the number of muons. The correlation of $X_{\max}$ and $\ln R_\mu$ is unaffected by a possible shift of the absolute scale of both $X_{\max}$ and $\ln R_\mu$ [26], as well as the bias correction described in Section 2.2. We investigate the correlation based on both the Pearson correlation coefficient, $\varrho(X,Y) = \mathrm{cov}[X,Y]/\sqrt{\mathrm{var}[X]\,\mathrm{var}[Y]}$, as well as the Gideon-Hollister rank correlation coefficient r_G [27]. The behaviour of r_G using simulations for various composition scenarios using the simulation library described in Section 2.2 is shown in Fig. 5 (*left/middle*). Proton, helium, oxygen, and iron primary particles are mixed at different ratios, where red (blue) markers represent a proton (iron) dominated proton-iron-only mix. Black markers represent other mixes of two primaries at different ratios, and gray markers indicate mixed scenarios including all four types of primaries. For each of the mixes the correlation of $X_{\max}$ and $\ln R_\mu$ is evaluated, with the energy-dependence of $X_{\max}$ removed assuming a linear elongation rate. In general, pure composition scenarios tend to produce only mildly anti-correlated $X_{\max}$ and $\ln R_\mu$ data, as can be seen from the four peaks in the "umbrella"-like plot of Fig. 5 (*left*). The strongest anti-correlation is observed for an extreme proton-iron-only mix at a ratio close[3] to 1:1.

The data interpreted in terms of r_G as a function of the primary energy show a strong anti-correlation around the *ankle* region [28], that is consistent with the results obtained in [25]. At ≈6 EeV, the value of r_G increases, which indicates a change in the composition of the primary beam. At higher primary energies the anti-correlation of $X_{\max}$ and $\ln R_\mu$ is consistent with pure and mixed composition scenarios. The data can be interpreted in the same way in terms of ϱ, which is, however, more sensitive to individual outliers.

[3]The strongest anti-correlation is observed for a proton-iron mix at a ratio of about $\frac{12}{10}$ to 1.

4. Summary and Conclusion

In this work, we present a method to estimate the number of muons in Auger hybrid events based on a combination of fluorescence and surface detector data above 3 EeV. When interpreting the surface detector data, the estimated primary energy as well as the depth of the shower maximum from the fluorescence detector data are taken into account. We present the number of muons as a function of the primary energy and confirm the result of previous analyses, indicating a significantly larger number of muons being produced in air showers than in simulations. The average number of muons is increasing with the primary energy, implying an increasingly heavier composition of cosmic rays. While the energy scale was identified as the main source of systematic uncertainties, a consistent interpretation of the mass composition using the number of muons and the depth of the shower maximum is not possible within experimental uncertainties. Furthermore, we present the correlation of the depth of the shower maximum and the number of muons as measured from individual events. We observe a strong anti-correlation around the ankle region, which is expected only from a mixed composition.

References

[1] R. Alves Batista et al., *Front. Astron. Space Sci.* **6** (2019) 23 [1903.06714].
[2] EAS-MSU, IceCube, KASCADE-Grande, NEVOD-DECOR, Pierre Auger, SUGAR, Telescope Array, Yakutsk EAS Array Collaboration, *PoS* **ICRC2021** (2021) 349 [2108.08341].
[3] Pierre Auger Collaboration, *Eur. Phys. J. C* **80** (2020) 751.
[4] Pierre Auger Collaboration, *Phys. Rev. Lett.* **126** (2021) 152002 [2102.07797].
[5] Pierre Auger Collaboration, *Nucl. Instrum. Meth. A* **798** (2015) 172 [1502.01323].
[6] J. Hersil, I. Escobar, D. Scott, G. Clark and S. Olbert, *Phys. Rev. Lett.* **6** (1961) 22.
[7] J. Alvarez-Muniz, R. Engel, T.K. Gaisser, J.A. Ortiz and T. Stanev, *Phys. Rev. D* **66** (2002) 123004 [astro-ph/0209117].
[8] M. Stadelmaier, M. Roth, D. Schmidt and D. Veberic, *Proc. Int. Cosmic Ray Conf.* **395** (2021) 432.
[9] D. Heck, J. Knapp, J. Capdevielle, G. Schatz, T. Thouw et al., *Report FZKA* **6019** (1998) .
[10] A.M. Hillas, *J. Phys. G* **8** (1982) 1461.
[11] P. Lipari, *Phys. Rev. D* **79** (2009) 063001 [0809.0190].
[12] S. Lafebre, R. Engel, H. Falcke, J. Horandel, T. Huege, J. Kuijpers et al., *Astropart. Phys.* **31** (2009) 243 [0902.0548].
[13] M. Ave, R. Engel, J. Gonzalez, D. Heck, T. Pierog and M. Roth, *Proc. Int. Cosmic Ray Conf.* **2** (2011) 178.
[14] M. Ave, R. Engel, M. Roth and A. Schulz, *Astropart. Phys.* **87** (2017) 23.
[15] K. Kamata and J. Nishimura, *Prog. Theor. Phys. Supplement* **6** (1958) 93.
[16] K. Greisen, *Ann. Rev. Nucl. Sci.* **10** (1960) 63.
[17] Pierre Auger Collaboration, *Nucl. Instrum. Meth. A* **568** (2006) 839 [2102.01656].
[18] T. Pierog, I. Karpenko, J.M. Katzy, E. Yatsenko and K. Werner, *Phys. Rev. C* **92** (2015) 034906.
[19] S. Argiro, S.L.C. Barroso, J. Gonzalez, L. Nellen, T.C. Paul, T.A. Porter et al., *Nucl. Instrum. Meth. A* **580** (2007) 1485 [0707.1652].
[20] R.S. Fletcher, T.K. Gaisser, P. Lipari and T. Stanev, *Phys. Rev. D* **50** (1994) 5710.
[21] S. Ostapchenko, *Phys. Rev. D* **83** (2011) 014018 [1010.1869].
[22] Pierre Auger Collaboration, *Phys. Rev. D* **90** (2014) 122005 [1409.4809].
[23] Pierre Auger Collaboration, *Phys. Rev. D* **102** (2020) 62005 [2008.06486].
[24] P. Younk and M. Risse, *Astropart. Phys.* **35** (2012) 807 [1203.3732].
[25] Pierre Auger Collaboration, *PoS* **ICRC2019** (2020) 482.
[26] Pierre Auger Collaboration, 2209.00744.
[27] R.A. Gideon and R.A. Hollister, *Journal of the American Statistical Association* **82** (1987) 656.
[28] Pierre Auger Collaboration, *Phys. Rev. Lett.* **125** (2020) 121106 [2008.06488].

The Pierre Auger Collaboration

A. Abdul Halim[13], P. Abreu[72], M. Aglietta[54,52], I. Allekotte[1], K. Almeida Cheminant[70], A. Almela[7,12], R. Aloisio[45,46], J. Alvarez-Muñiz[79], J. Ammerman Yebra[79], G.A. Anastasi[54,52], L. Anchordoqui[86], B. Andrada[7], S. Andringa[72], C. Aramo[50], P.R. Araújo Ferreira[42], E. Arnone[63,52], J. C. Arteaga Velázquez[67], H. Asorey[7], P. Assis[72], G. Avila[11], E. Avocone[57,46], A.M. Badescu[75], A. Bakalova[32], A. Balaceanu[73], F. Barbato[45,46], A. Bartz Mocellin[85], J.A. Bellido[13,69], C. Berat[36], M.E. Bertaina[63,52], G. Bhatta[70], M. Bianciotto[63,52], P.L. Biermann[h], V. Binet[5], K. Bismark[39,7], T. Bister[80,81], J. Biteau[37], J. Blazek[32], C. Bleve[36], J. Blümer[41], M. Boháčová[32], D. Boncioli[57,46], C. Bonifazi[8,26], L. Bonneau Arbeletche[21], N. Borodai[70], J. Brack[j], P.G. Brichetto Orchera[7], F.L. Briechle[42], A. Bueno[78], S. Buitink[15], M. Buscemi[47,61], M. Büsken[39,7], A. Bwembya[80,81], K.S. Caballero-Mora[66], S. Cabana-Freire[79], L. Caccianiga[59,49], I. Caracas[38], R. Caruso[58,47], A. Castellina[54,52], F. Catalani[18], G. Cataldi[48], L. Cazon[79], M. Cerda[10], A. Cermenati[45,46], J.A. Chinellato[21], J. Chudoba[32], L. Chytka[33], R.W. Clay[13], A.C. Cobos Cerutti[6], R. Colalillo[60,50], A. Coleman[90], M.R. Coluccia[48], R. Conceição[72], A. Condorelli[37], G. Consolati[49,55], M. Conte[56,48], F. Convenga[41], D. Correia dos Santos[28], P.J. Costa[72], C.E. Covault[84], M. Cristinziani[44], C.S. Cruz Sanchez[3], S. Dasso[4,2], K. Daumiller[41], B.R. Dawson[13], R.M. de Almeida[28], J. de Jesús[7,41], S.J. de Jong[80,81], J.R.T. de Mello Neto[26,27], I. De Mitri[45,46], J. de Oliveira[17], D. de Oliveira Franco[21], F. de Palma[56,48], V. de Souza[19], E. De Vito[56,48], A. Del Popolo[58,47], O. Deligny[34], N. Denner[32], L. Deval[41,7], A. di Matteo[52], M. Dobre[73], C. Dobrigkeit[21], J.C. D'Olivo[68], L.M. Domingues Mendes[72], J.C. dos Anjos, R.C. dos Anjos[25], J. Ebr[32], F. Ellwanger[41], M. Emam[80,81], R. Engel[39,41], I. Epicoco[56,48], M. Erdmann[42], A. Etchegoyen[7,12], C. Evoli[45,46], H. Falcke[80,82,81], J. Farmer[89], G. Farrar[88], A.C. Fauth[21], N. Fazzini[e], F. Feldbusch[40], F. Fenu[41,d], A. Fernandes[72], B. Fick[87], J.M. Figueira[7], A. Filipčič[77,76], T. Fitoussi[41], B. Flaggs[90], T. Fodran[80], T. Fujii[89,f], A. Fuster[7,12], C. Galea[80], C. Galelli[59,49], B. García[6], C. Gaudu[38], H. Gemmeke[40], F. Gesualdi[7,41], A. Gherghel-Lascu[73], P.L. Ghia[34], U. Giaccari[48], M. Giammarchi[49], J. Glombitza[42,g], F. Gobbi[10], F. Gollan[7], G. Golup[1], M. Gómez Berisso[1], P.F. Gómez Vitale[11], J.P. Gongora[11], J.M. González[1], N. González[7], I. Goos[1], D. Góra[70], A. Gorgi[54,52], M. Gottowik[79], T.D. Grubb[13], F. Guarino[60,50], G.P. Guedes[22], E. Guido[44], S. Hahn[39], P. Hamal[32], M.R. Hampel[7], P. Hansen[3], D. Harari[1], V.M. Harvey[13], A. Haungs[41], T. Hebbeker[42], C. Hojvat[e], J.R. Hörandel[80,81], P. Horvath[33], M. Hrabovský[33], T. Huege[41,15], A. Insolia[58,47], P.G. Isar[74], P. Janecek[32], J.A. Johnsen[85], J. Jurysek[32], A. Kääpä[38], K.H. Kampert[38], B. Keilhauer[41], A. Khakurdikar[80], V.V. Kizakke Covilakam[7,41], H.O. Klages[41], M. Kleifges[40], F. Knapp[39], N. Kunka[40], B.L. Lago[16], N. Langner[42], M.A. Leigui de Oliveira[24], Y Lema-Capeans[79], V. Lenok[39], A. Letessier-Selvon[35], I. Lhenry-Yvon[34], D. Lo Presti[58,47], L. Lopes[72], L. Lu[91], Q. Luce[39], J.P. Lundquist[76], A. Machado Payeras[21], M. Majercakova[32], D. Mandat[32], B.C. Manning[13], P. Mantsch[e], S. Marafico[34], F.M. Mariani[59,49], A.G. Mariazzi[3], I.C. Mariş[14], G. Marsella[61,47], D. Martello[56,48], S. Martinelli[41,7], O. Martínez Bravo[64], M.A. Martins[79], M. Mastrodicasa[57,46], H.J. Mathes[41], J. Matthews[a], G. Matthiae[62,51], E. Mayotte[85,38], S. Mayotte[85], P.O. Mazur[e], G. Medina-Tanco[68], J. Meinert[38], D. Melo[7], A. Menshikov[40], C. Merx[41], S. Michal[33], M.I. Micheletti[5], L. Miramonti[59,49], S. Mollerach[1], F. Montanet[36], L. Morejon[38], C. Morello[54,52], A.L. Müller[32], K. Mulrey[80,81], R. Mussa[52], M. Muzio[88], W.M. Namasaka[38], S. Negi[32], L. Nellen[68], K. Nguyen[87], G. Nicora[9], M. Niculescu-Oglinzanu[73], M. Niechciol[44], D. Nitz[87], D. Nosek[31], V. Novotny[31], L. Nožka[33], A Nucita[56,48], L.A. Núñez[30], C. Oliveira[19], M. Palatka[32], J. Pallotta[9], S. Panja[32], G. Parente[79], T. Paulsen[38], J. Pawlowsky[38], M. Pech[32], J. Pękala[70], R. Pelayo[65], L.A.S. Pereira[23], E.E. Pereira Martins[39,7], J. Perez Armand[20], C. Pérez Bertolli[7,41], L. Perrone[56,48], S. Petrera[45,46], C. Petrucci[57,46], T. Pierog[41], M. Pimenta[72], M. Platino[7], B. Pont[80], M. Pothast[81,80], M. Pourmohammad Shahvar[61,47], P. Privitera[89], M. Prouza[32], A. Puyleart[87], S. Querchfeld[38], J. Rautenberg[38], D. Ravignani[7], M. Reininghaus[39], J. Ridky[32], F. Riehn[79], M. Risse[44], V. Rizi[57,46], W. Rodrigues de Carvalho[80], E. Rodriguez[7,41], J. Rodriguez Rojo[11], M.J. Roncoroni[7], S. Rossoni[43], M. Roth[41], E. Roulet[1], A.C. Rovero[4], P. Ruehl[44], A. Saftoiu[73], M. Saharan[80], F. Salamida[57,46], H. Salazar[64], G. Salina[51], J.D. Sanabria Gomez[30], F. Sánchez[7], E.M. Santos[20], E. Santos[32],

F. Sarazin[85], R. Sarmento[72], R. Sato[11], P. Savina[91], C.M. Schäfer[41], V. Scherini[56,48], H. Schieler[41], M. Schimassek[34], M. Schimp[38], F. Schlüter[41], D. Schmidt[39], O. Scholten[15,i], H. Schoorlemmer[80,81], P. Schovánek[32], F.G. Schröder[90,41], J. Schulte[42], T. Schulz[41], S.J. Sciutto[3], M. Scornavacche[7,41], A. Segreto[53,47], S. Sehgal[38], S.U. Shivashankara[76], G. Sigl[43], G. Silli[7], O. Sima[73,b], F. Simon[40], R. Smau[73], R. Šmída[89], P. Sommers[k], J.F. Soriano[86], R. Squartini[10], M. Stadelmaier[32], D. Stanca[73], S. Stanič[76], J. Stasielak[70], P. Stassi[36], S. Strähnz[39], M. Straub[42], M. Suárez-Durán[14], T. Suomijärvi[37], A.D. Supanitsky[7], Z. Svozilikova[32], Z. Szadkowski[71], A. Tapia[29], C. Taricco[63,52], C. Timmermans[81,80], O. Tkachenko[41], P. Tobiska[32], C.J. Todero Peixoto[18], B. Tomé[72], Z. Torrès[36], A. Travaini[10], P. Travnicek[32], C. Trimarelli[57,46], M. Tueros[3], M. Unger[41], L. Vaclavek[33], M. Vacula[33], J.F. Valdés Galicia[68], L. Valore[60,50], E. Varela[64], A. Vásquez-Ramírez[30], D. Veberič[41], C. Ventura[27], I.D. Vergara Quispe[3], V. Verzi[51], J. Vicha[32], J. Vink[83], J. Vlastimil[32], S. Vorobiov[76], C. Watanabe[26], A.A. Watson[c], A. Weindl[41], L. Wiencke[85], H. Wilczyński[70], D. Wittkowski[38], B. Wundheiler[7], B. Yue[38], A. Yushkov[32], O. Zapparrata[14], E. Zas[79], D. Zavrtanik[76,77], M. Zavrtanik[77,76]

[1] Centro Atómico Bariloche and Instituto Balseiro (CNEA-UNCuyo-CONICET), San Carlos de Bariloche, Argentina
[2] Departamento de Física and Departamento de Ciencias de la Atmósfera y los Océanos, FCEyN, Universidad de Buenos Aires and CONICET, Buenos Aires, Argentina
[3] IFLP, Universidad Nacional de La Plata and CONICET, La Plata, Argentina
[4] Instituto de Astronomía y Física del Espacio (IAFE, CONICET-UBA), Buenos Aires, Argentina
[5] Instituto de Física de Rosario (IFIR) – CONICET/U.N.R. and Facultad de Ciencias Bioquímicas y Farmacéuticas U.N.R., Rosario, Argentina
[6] Instituto de Tecnologías en Detección y Astropartículas (CNEA, CONICET, UNSAM), and Universidad Tecnológica Nacional – Facultad Regional Mendoza (CONICET/CNEA), Mendoza, Argentina
[7] Instituto de Tecnologías en Detección y Astropartículas (CNEA, CONICET, UNSAM), Buenos Aires, Argentina
[8] International Center of Advanced Studies and Instituto de Ciencias Físicas, ECyT-UNSAM and CONICET, Campus Miguelete – San Martín, Buenos Aires, Argentina
[9] Laboratorio Atmósfera – Departamento de Investigaciones en Láseres y sus Aplicaciones – UNIDEF (CITEDEF-CONICET), Argentina
[10] Observatorio Pierre Auger, Malargüe, Argentina
[11] Observatorio Pierre Auger and Comisión Nacional de Energía Atómica, Malargüe, Argentina
[12] Universidad Tecnológica Nacional – Facultad Regional Buenos Aires, Buenos Aires, Argentina
[13] University of Adelaide, Adelaide, S.A., Australia
[14] Université Libre de Bruxelles (ULB), Brussels, Belgium
[15] Vrije Universiteit Brussels, Brussels, Belgium
[16] Centro Federal de Educação Tecnológica Celso Suckow da Fonseca, Petropolis, Brazil
[17] Instituto Federal de Educação, Ciência e Tecnologia do Rio de Janeiro (IFRJ), Brazil
[18] Universidade de São Paulo, Escola de Engenharia de Lorena, Lorena, SP, Brazil
[19] Universidade de São Paulo, Instituto de Física de São Carlos, São Carlos, SP, Brazil
[20] Universidade de São Paulo, Instituto de Física, São Paulo, SP, Brazil
[21] Universidade Estadual de Campinas, IFGW, Campinas, SP, Brazil
[22] Universidade Estadual de Feira de Santana, Feira de Santana, Brazil
[23] Universidade Federal de Campina Grande, Centro de Ciencias e Tecnologia, Campina Grande, Brazil
[24] Universidade Federal do ABC, Santo André, SP, Brazil
[25] Universidade Federal do Paraná, Setor Palotina, Palotina, Brazil
[26] Universidade Federal do Rio de Janeiro, Instituto de Física, Rio de Janeiro, RJ, Brazil
[27] Universidade Federal do Rio de Janeiro (UFRJ), Observatório do Valongo, Rio de Janeiro, RJ, Brazil
[28] Universidade Federal Fluminense, EEIMVR, Volta Redonda, RJ, Brazil
[29] Universidad de Medellín, Medellín, Colombia
[30] Universidad Industrial de Santander, Bucaramanga, Colombia

PoS(ICRC2023)339

[31] Charles University, Faculty of Mathematics and Physics, Institute of Particle and Nuclear Physics, Prague, Czech Republic
[32] Institute of Physics of the Czech Academy of Sciences, Prague, Czech Republic
[33] Palacky University, Olomouc, Czech Republic
[34] CNRS/IN2P3, IJCLab, Université Paris-Saclay, Orsay, France
[35] Laboratoire de Physique Nucléaire et de Hautes Energies (LPNHE), Sorbonne Université, Université de Paris, CNRS-IN2P3, Paris, France
[36] Univ. Grenoble Alpes, CNRS, Grenoble Institute of Engineering Univ. Grenoble Alpes, LPSC-IN2P3, 38000 Grenoble, France
[37] Université Paris-Saclay, CNRS/IN2P3, IJCLab, Orsay, France
[38] Bergische Universität Wuppertal, Department of Physics, Wuppertal, Germany
[39] Karlsruhe Institute of Technology (KIT), Institute for Experimental Particle Physics, Karlsruhe, Germany
[40] Karlsruhe Institute of Technology (KIT), Institut für Prozessdatenverarbeitung und Elektronik, Karlsruhe, Germany
[41] Karlsruhe Institute of Technology (KIT), Institute for Astroparticle Physics, Karlsruhe, Germany
[42] RWTH Aachen University, III. Physikalisches Institut A, Aachen, Germany
[43] Universität Hamburg, II. Institut für Theoretische Physik, Hamburg, Germany
[44] Universität Siegen, Department Physik – Experimentelle Teilchenphysik, Siegen, Germany
[45] Gran Sasso Science Institute, L'Aquila, Italy
[46] INFN Laboratori Nazionali del Gran Sasso, Assergi (L'Aquila), Italy
[47] INFN, Sezione di Catania, Catania, Italy
[48] INFN, Sezione di Lecce, Lecce, Italy
[49] INFN, Sezione di Milano, Milano, Italy
[50] INFN, Sezione di Napoli, Napoli, Italy
[51] INFN, Sezione di Roma "Tor Vergata", Roma, Italy
[52] INFN, Sezione di Torino, Torino, Italy
[53] Istituto di Astrofisica Spaziale e Fisica Cosmica di Palermo (INAF), Palermo, Italy
[54] Osservatorio Astrofisico di Torino (INAF), Torino, Italy
[55] Politecnico di Milano, Dipartimento di Scienze e Tecnologie Aerospaziali , Milano, Italy
[56] Università del Salento, Dipartimento di Matematica e Fisica "E. De Giorgi", Lecce, Italy
[57] Università dell'Aquila, Dipartimento di Scienze Fisiche e Chimiche, L'Aquila, Italy
[58] Università di Catania, Dipartimento di Fisica e Astronomia "Ettore Majorana", Catania, Italy
[59] Università di Milano, Dipartimento di Fisica, Milano, Italy
[60] Università di Napoli "Federico II", Dipartimento di Fisica "Ettore Pancini", Napoli, Italy
[61] Università di Palermo, Dipartimento di Fisica e Chimica "E. Segrè", Palermo, Italy
[62] Università di Roma "Tor Vergata", Dipartimento di Fisica, Roma, Italy
[63] Università Torino, Dipartimento di Fisica, Torino, Italy
[64] Benemérita Universidad Autónoma de Puebla, Puebla, México
[65] Unidad Profesional Interdisciplinaria en Ingeniería y Tecnologías Avanzadas del Instituto Politécnico Nacional (UPIITA-IPN), México, D.F., México
[66] Universidad Autónoma de Chiapas, Tuxtla Gutiérrez, Chiapas, México
[67] Universidad Michoacana de San Nicolás de Hidalgo, Morelia, Michoacán, México
[68] Universidad Nacional Autónoma de México, México, D.F., México
[69] Universidad Nacional de San Agustin de Arequipa, Facultad de Ciencias Naturales y Formales, Arequipa, Peru
[70] Institute of Nuclear Physics PAN, Krakow, Poland
[71] University of Łódź, Faculty of High-Energy Astrophysics,Łódź, Poland
[72] Laboratório de Instrumentação e Física Experimental de Partículas – LIP and Instituto Superior Técnico – IST, Universidade de Lisboa – UL, Lisboa, Portugal
[73] "Horia Hulubei" National Institute for Physics and Nuclear Engineering, Bucharest-Magurele, Romania
[74] Institute of Space Science, Bucharest-Magurele, Romania
[75] University Politehnica of Bucharest, Bucharest, Romania
[76] Center for Astrophysics and Cosmology (CAC), University of Nova Gorica, Nova Gorica, Slovenia
[77] Experimental Particle Physics Department, J. Stefan Institute, Ljubljana, Slovenia

PoS(ICRC2023)339

[78] Universidad de Granada and C.A.F.P.E., Granada, Spain
[79] Instituto Galego de Física de Altas Enerxías (IGFAE), Universidade de Santiago de Compostela, Santiago de Compostela, Spain
[80] IMAPP, Radboud University Nijmegen, Nijmegen, The Netherlands
[81] Nationaal Instituut voor Kernfysica en Hoge Energie Fysica (NIKHEF), Science Park, Amsterdam, The Netherlands
[82] Stichting Astronomisch Onderzoek in Nederland (ASTRON), Dwingeloo, The Netherlands
[83] Universiteit van Amsterdam, Faculty of Science, Amsterdam, The Netherlands
[84] Case Western Reserve University, Cleveland, OH, USA
[85] Colorado School of Mines, Golden, CO, USA
[86] Department of Physics and Astronomy, Lehman College, City University of New York, Bronx, NY, USA
[87] Michigan Technological University, Houghton, MI, USA
[88] New York University, New York, NY, USA
[89] University of Chicago, Enrico Fermi Institute, Chicago, IL, USA
[90] University of Delaware, Department of Physics and Astronomy, Bartol Research Institute, Newark, DE, USA
[91] University of Wisconsin-Madison, Department of Physics and WIPAC, Madison, WI, USA

—

[a] Louisiana State University, Baton Rouge, LA, USA
[b] also at University of Bucharest, Physics Department, Bucharest, Romania
[c] School of Physics and Astronomy, University of Leeds, Leeds, United Kingdom
[d] now at Agenzia Spaziale Italiana (ASI). Via del Politecnico 00133, Roma, Italy
[e] Fermi National Accelerator Laboratory, Fermilab, Batavia, IL, USA
[f] now at Graduate School of Science, Osaka Metropolitan University, Osaka, Japan
[g] now at ECAP, Erlangen, Germany
[h] Max-Planck-Institut für Radioastronomie, Bonn, Germany
[i] also at Kapteyn Institute, University of Groningen, Groningen, The Netherlands
[j] Colorado State University, Fort Collins, CO, USA
[k] Pennsylvania State University, University Park, PA, USA

Acknowledgments

The successful installation, commissioning, and operation of the Pierre Auger Observatory would not have been possible without the strong commitment and effort from the technical and administrative staff in Malargüe. We are very grateful to the following agencies and organizations for financial support:

Argentina – Comisión Nacional de Energía Atómica; Agencia Nacional de Promoción Científica y Tecnológica (ANPCyT); Consejo Nacional de Investigaciones Científicas y Técnicas (CONICET); Gobierno de la Provincia de Mendoza; Municipalidad de Malargüe; NDM Holdings and Valle Las Leñas; in gratitude for their continuing cooperation over land access; Australia – the Australian Research Council; Belgium – Fonds de la Recherche Scientifique (FNRS); Research Foundation Flanders (FWO); Brazil – Conselho Nacional de Desenvolvimento Científico e Tecnológico (CNPq); Financiadora de Estudos e Projetos (FINEP); Fundação de Amparo à Pesquisa do Estado de Rio de Janeiro (FAPERJ); São Paulo Research Foundation (FAPESP) Grants No. 2019/10151-2, No. 2010/07359-6 and No. 1999/05404-3; Ministério da Ciência, Tecnologia, Inovações e Comunicações (MCTIC); Czech Republic – Grant No. MSMT CR LTT18004, LM2015038, LM2018102, CZ.02.1.01/0.0/0.0/16_013/0001402, CZ.02.1.01/0.0/0.0/18_046/0016010 and CZ.02.1.01/0.0/0.0/17_049/0008422; France – Centre de Calcul IN2P3/CNRS; Centre National de la Recherche Scientifique (CNRS); Conseil Régional Ile-de-France; Département Physique Nucléaire et Corpusculaire (PNC-IN2P3/CNRS); Département Sciences de l'Univers (SDU-INSU/CNRS); Institut Lagrange de Paris (ILP) Grant No. LABEX ANR-10-LABX-63 within the Investissements d'Avenir Programme Grant No. ANR-11-IDEX-0004-02; Germany – Bundesministerium für Bildung und Forschung (BMBF); Deutsche Forschungsgemeinschaft (DFG); Finanzministerium Baden-Württemberg; Helmholtz Alliance for Astroparticle Physics (HAP); Helmholtz-Gemeinschaft Deutscher Forschungszentren (HGF); Ministerium für Kultur und Wissenschaft des Landes Nordrhein-Westfalen; Ministerium für Wissenschaft, Forschung und Kunst des Landes Baden-Württemberg; Italy – Istituto Nazionale di Fisica Nucleare (INFN); Istituto Nazionale di Astrofisica (INAF); Ministero dell'Universitá e della Ricerca (MUR); CETEMPS Center of Excellence; Ministero degli Affari Esteri (MAE), ICSC Centro Nazionale di Ricerca in High Performance Computing, Big Data

and Quantum Computing, funded by European Union NextGenerationEU, reference code CN_00000013; México – Consejo Nacional de Ciencia y Tecnología (CONACYT) No. 167733; Universidad Nacional Autónoma de México (UNAM); PAPIIT DGAPA-UNAM; The Netherlands – Ministry of Education, Culture and Science; Netherlands Organisation for Scientific Research (NWO); Dutch national e-infrastructure with the support of SURF Cooperative; Poland – Ministry of Education and Science, grants No. DIR/WK/2018/11 and 2022/WK/12; National Science Centre, grants No. 2016/22/M/ST9/00198, 2016/23/B/ST9/01635, 2020/39/B/ST9/01398, and 2022/45/B/ST9/02163; Portugal – Portuguese national funds and FEDER funds within Programa Operacional Factores de Competitividade through Fundação para a Ciência e a Tecnologia (COMPETE); Romania – Ministry of Research, Innovation and Digitization, CNCS-UEFISCDI, contract no. 30N/2023 under Romanian National Core Program LAPLAS VII, grant no. PN 23 21 01 02 and project number PN-III-P1-1.1-TE-2021-0924/TE57/2022, within PNCDI III; Slovenia – Slovenian Research Agency, grants P1-0031, P1-0385, I0-0033, N1-0111; Spain – Ministerio de Economía, Industria y Competitividad (FPA2017-85114-P and PID2019-104676GB-C32), Xunta de Galicia (ED431C 2017/07), Junta de Andalucía (SOMM17/6104/UGR, P18-FR-4314) Feder Funds, RENATA Red Nacional Temática de Astropartículas (FPA2015-68783-REDT) and María de Maeztu Unit of Excellence (MDM-2016-0692); USA – Department of Energy, Contracts No. DE-AC02-07CH11359, No. DE-FR02-04ER41300, No. DE-FG02-99ER41107 and No. DE-SC0011689; National Science Foundation, Grant No. 0450696; The Grainger Foundation; Marie Curie-IRSES/EPLANET; European Particle Physics Latin American Network; and UNESCO.